



Nondestructive and active interrogation system for special nuclear material: proof of principle and initial results

Mahmoud Bakr^{1,2,3,6} · Kai Masuda¹ · Yoshiyuki Takahashi⁴ · Tsuyoshi Misawa⁴ · Norio Yamakawa⁵ · Tomas Scott²

Received: 2 September 2023 / Revised: 1 November 2023 / Accepted: 3 November 2023 / Published online: 31 May 2024
© The Author(s) 2024

Abstract

Herein, we employ the threshold energy neutron analysis (TENA) technique to introduce the world's first active interrogation system to detect special nuclear materials (SNMs), including U-235 and Pu-239. The system utilizes a DD neutron generator based on inertial electrostatic confinement (IEC) to interrogate suspicious objects. To detect secondary neutrons produced during fission reactions induced in SNMs, a tensioned metastable fluid detector (TMFD) is employed. The current status of the system's development is reported in this paper, accompanied by the results from experiments conducted to detect 10 g of highly enriched uranium (HEU). Notably, the experimental findings demonstrate a distinct difference in the count rates of measurements with and without HEU. This difference in count rates surpasses two times the standard deviation, indicating a confidence level of more than 96% for identifying the presence of HEU. The paper presents and extensively discusses the proof-of-principle experimental results, along with the system's planned trajectory.

Keywords Special nuclear materials · Uranium detection · Inertial electrostatic confinement fusion · TENA · HEU · CTMFD

This builds upon past work supported by Special Coordination Funds for Promoting Science and Technology, sponsored by Japan's Ministry of Education, Culture, Sports, Science and Technology (MEXT). Assistance and advice from Prof. Rusi Taleyakhan and his research group members at Purdue University and Sagamore Adams Laboratories LLC are all highly acknowledged.

✉ Mahmoud Bakr
Mahmoud.bakrarby@bristol.ac.uk

¹ Institute of Advanced Energy, Kyoto University, Gokasho, Uji, Kyoto 611-0011, Japan

² School of Physics, University of Bristol, Bs81TL Tyndall Avenue, Bristol, UK

³ Physics Department, Faculty of Science, Assiut University, Assiut 71516, Egypt

⁴ Research Reactor Institute, Kyoto University, 2 Asashiro-Nishi, Kumatori, Osaka 590-0494, Japan

⁵ Pony Industry Co. Ltd., 2-3-6 Kitakyuhoji-Machi, Chuo-Ku, Osaka 541-0057, Japan

⁶ Astral Neutronics LTD, Unit H5, Hallen, Bristol BS10 7SB, UK

1 Introduction

Nondestructive inspection systems play a crucial role in preventing terrorist threats and the illicit smuggling of special nuclear materials (SNM) at ports and seaports [1]. For many years, nuclear security in various countries has predominantly focused on the investigation of SNMs, particularly Pu-239 and U-235 [2]. Numerous passive and active interrogation methods have been developed and implemented at ports and seaports worldwide to investigate SNM [1–7]. Passive detection systems, which seek emitted neutrons and/or photons, prove effective for investigating SNM with a distinct spontaneous fission signature, such as Pu-239. However, these methods prove insufficient for detecting highly enriched uranium (HEU) concealed within shielding materials due to its weak spontaneous fission signature. Conversely, active interrogation systems utilize probing neutrons and/or photons and subsequently analyze secondary emissions to investigate SNM. These systems hold promise for detecting HEU concealed within shielded and unshielded containers. Nevertheless, the induced fission signature resulting from probing neutrons or photons can be challenging to distinguish due to ambiguity in neutrons' energy and

intensity, making differentiation between probing and fission neutrons difficult [8].

Energetic gamma (γ)-rays, with their high penetration capabilities through shielding materials and selective interactions, show great promise as tools for investigating SNMs. Various inspection methods have been developed and employed, utilizing the detection of nuclear resonance fluorescence (NRF) induced by light for interrogation [1, 9, 10]. However, interference between probing and fission photons during the investigation makes the interrogation process complex and challenging to distinguish. Therefore, sophisticated analysis techniques are necessary. Similarly, neutrons possess unique characteristics for SNM interrogations due to their chargeless nature and penetration capabilities. Using thermalized D–T (deuterium–tritium) neutrons, initially at 14.01 MeV before moderation, for SNM investigation results in an induced fission signature of neutrons and/or γ -rays, allowing the identification of fissile materials using various developed and applied analysis methods. These methods include the delayed neutron analysis method [11], differential die-away analysis [12], noise analysis method [13], and neutron rotation method [14, 15]. High-intensity D–T neutron sources, operated in pulsed mode, are essential for these methods. However, the signal-to-noise ratio in these techniques poses challenges to precisely detect fissile materials concealed inside shielded containers. Additionally, issues, such as operations, maintenance, safety concerns, and the shortage of tritium, render large-scale adoption of D–T neutron sources for SNM interrogations complex.

To address these challenges, it is crucial to search for alternative neutron sources and implement intelligent detection techniques for SNM that can overcome the complications associated with current detection methods.

This pursuit is vital for enhancing nuclear security worldwide. The present paper introduces a novel approach that combines a D–D neutron source based on an inertial electrostatic confinement (IEC) fusion device [16] with the centrifugally tensioned metastable fluid detector (C-TMFD) [17], which is utilized in the threshold energy neutron analysis (TENA) technique [18] to detect the secondary neutrons from HEU. The proposed method involves using 2.45 MeV probing neutrons to interrogate the HEU material, and the resulting fission neutrons are detected using the C-TMFD. The system's design aims to interrogate 1000 g of HEU concealed within a $1\text{ m} \times 1\text{ m} \times 1\text{ m}$ cargo without any shielding around the HEU. To demonstrate the proof of principle, a preliminary test is conducted in this study, where only 10 g of HEU impeded in a natural uranium is subjected to interrogation using the proposed technique.

The paper is structured as follows: Sect. 2 presents the methods and tools used, including details about the neutron source and detector, along with the detection method. Section 3 provides the experimental layout and conditions. The preliminary results and ensuing discussion are presented in Sect. 4. Finally, Sect. 5 offers a summary of the findings and outlines potential future work.

2 Methods and tools

2.1 IEC neutron generator

The IEC fusion system, in its fundamental configuration, consists of a negative bias concentric grid cathode encircled by a grounded anode within a vacuum chamber, as illustrated in Fig. 1a [19–23]. A potential well is established by applying several tens of kilovolts of voltage between the

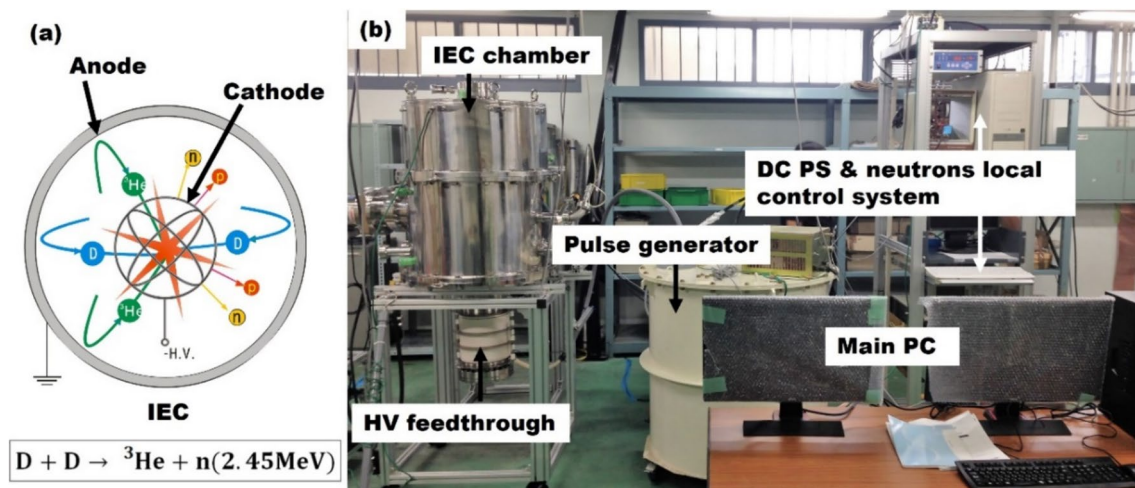


Fig. 1 (Color online) Diagram of the IEC fusion chamber (a), photograph of the IEC apparatus with the control system used for the HEU detection

cathode and the anode, and several tens of milliamps of current facilitating the ionization of fuels such as deuterium (D) and/or tritium (T) within the vacuum chamber. Initiating the discharge by applying tens of milliamps of current induces fusion reactions and the generation of neutrons. IEC fusion devices offer various advantages, including a straightforward configuration, the potential for steady-state (DC) or pulsed operation modes, ease of handling, and low start-up and maintenance costs. Consequently, they have garnered attention as neutron sources for diverse scientific research and industrial applications worldwide [24–31].

For the current experiment, an IEC with a 20 cm-diameter molybdenum cathode and a 56-cm-diameter stainless steel anode is employed, assembled within a 60-cm-diameter cylindrical vacuum chamber, as depicted in Fig. 1b [32]. Operating in a pulsed mode, the IEC neutron source produces monoenergetic D-D neutrons with an energy of 2.45 MeV. The system has a repetition rate of 10 Hz, a pulse width of approximately 120 μ s, and an average neutron production rate of approximately 3×10^5 n/s. The IEC device can be considered a volumetric neutron source, with neutron production peaking around the central cathode due to the expected highest energy of deuterium ions in this central region.

2.2 Fission neutron detector C-TMFD

The C-TMFD comprises a diamond-shaped glass pipe enclosure filled with a detection liquid and connected to a motor with adjustable speed, as illustrated in Fig. 2a [17]. In this study, decafluoropentane ($C_5H_2F_{10}$) serves as the detection liquid within the C-TMFD sensors. When the variable-speed motor rotates the diamond-shaped glass enclosure, it induces tension in the liquid, causing it to enter a state of tensioned metastability. This phenomenon occurs because the fluid experiences negative pressure near

the rotation axis due to the generated centrifugal force. The resulting tension, denoted as $p_{\text{neg}}(r)$, is a function of the radial position r relative to the rotation axis and can be calculated using Eq. (1):

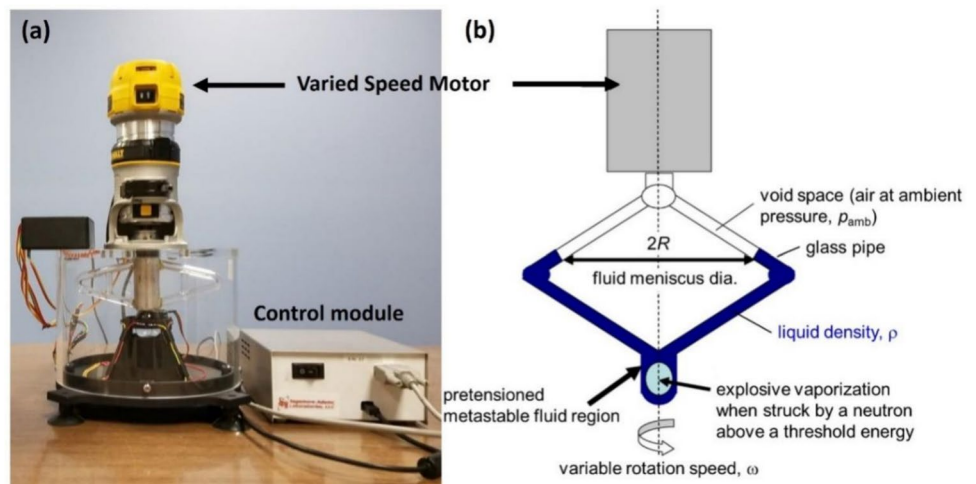
$$p_{\text{neg}}(r) = \frac{1}{2} \rho (R - r)^2 \omega^2 - p_{\text{amb}}, \quad (1)$$

where ρ represents the density of the liquid, R is the meniscus radius (as shown in Fig. 2b), ω stands for the rotation speed, and p_{amb} indicates the ambient pressure. Additional information can be found in other references [2, 17] for a more comprehensive understanding of this phenomenon. When an energetic neutron interacts with the active liquid inside the C-TMFD, the tensioned metastable liquid undergoes a transition to a stable gaseous state, resulting in localized explosive vaporization. An infrared sensor integrated into the enclosure wall of the C-TMFD detects this cavitation process and records the associated signals. The shift from the metastable liquid phase to the stable gas phase is initiated by a specific recoil energy transfer from the incident neutron to the molecules within the tensioned liquid. Consequently, neutrons with energies below a certain threshold can be selectively filtered out. Adjusting the rotation speed ω in Eq. (1) can modify this threshold energy. Furthermore, it is essential to note that the C-TMFD is entirely immune to gamma rays generated during the discharge of the IEC device, as further elucidated in the Ref. [2].

2.3 The TENA detection method

The TENA method is based on the neutron-in neutron-out technique, wherein the IEC device generates probing neutrons, and the C-TMFD serves to detect fission neutrons (secondary neutrons) emitted from the SNM, as illustrated in Fig. 3a. When SNM is impacted by thermal and/or epithermal neutrons originating from DD fusion (2.45 MeV),

Fig. 2 (Color online) A photograph of the C-TMFD utilized in the current experiment (a) and a schematic cross section (b) [17]



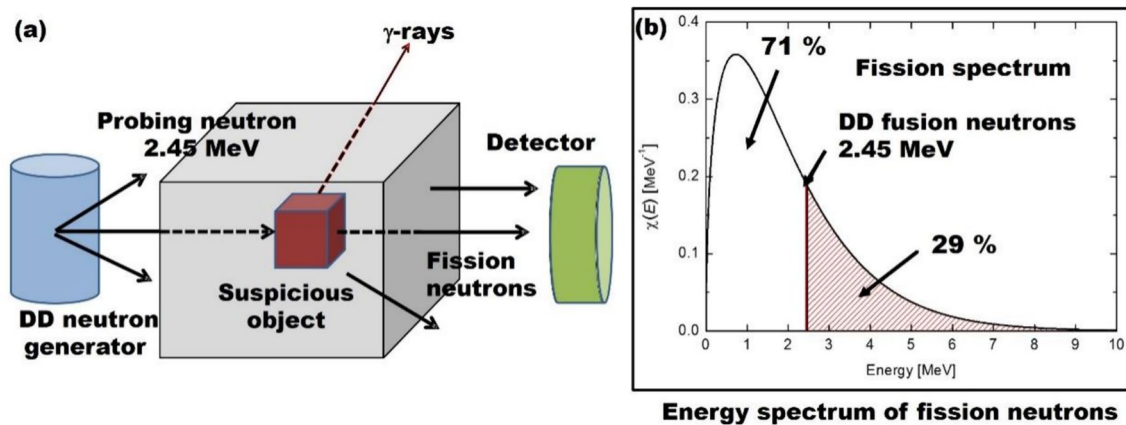


Fig. 3 (Color online) **a** Principle of the detection technique based on the TENA method and **b** neutron energy spectra from fission and DD neutron source

fission reactions occur inside the SNM, generating secondary neutrons. Approximately 70% of these secondary neutrons from SNMs have energies below that of DD neutrons, while the remaining 30% have energies above this threshold, as shown in Fig. 3b. Detecting neutrons with energies above 2.45 MeV, constituting approximately 30% of all secondary neutrons, serves as a distinctive signature for unambiguously identifying SNMs. This is because scattering tends to lower the probing neutron energies, making the presence of neutrons above the 2.45 MeV threshold energy unique to SNMs (excluding cosmic rays).

Earlier experimental studies employing a Cf-252 source as a simulant instead of HEU [18, 33] demonstrated the TENA method's capability to detect HEU while also revealing a challenge in constructing a TENA-based system. In this experiment, neutron spectrum measurements under three distinct conditions were performed, each designed to shed light on specific aspects of the research. First, the counts from the DD neutron source were measured to examine its spectral characteristics independently. Second, the counts from a separate Cf-252 neutron source were measured, leveraging its energy spectrum similarity to that of U-235 fission reactions, making it a suitable surrogate for fissile materials in the experiments. Lastly, the DD and Cf-252 neutron sources were combined to investigate their combined effects, providing valuable insights into scenarios where multiple neutron sources might interact. These carefully designed measurement scenarios allow us to comprehensively understand neutron interactions and spectral outcomes critical to the research objectives.

Figure 4a illustrates the distribution of measured count rates obtained from the liquid organic scintillator. This figure depicts the count rates resulting from three distinct sources: (i) DD neutrons originating from an IEC source, (ii) counts originating from a Cf-252 source, and (iii) counts obtained

when both IEC and Cf-252 sources are active simultaneously. The vertical dotted line within the figure serves as an indicator, marking the energy threshold corresponding to 2.45 MeV; this corresponds to DD neutrons emitted by the IEC source. For a more comprehensive description of the experimental setup, please refer to reference [14]. A noticeable distinction can be observed in the figure between the scenarios involving both the Cf-252 and DD source (represented by green dots) and the case with DD alone (represented by black dots) above the threshold energy. Of particular significance is the observation that the background count rates (black dots) above the threshold energy are considerably higher than those attributed to cosmic rays. These false positive signals may arise from two possible sources: first, neutron-induced γ -rays, and second, neutron accumulation below the threshold. In the latter scenario, multiple neutrons incident within the detector's response time, while below the threshold, can combine to generate a signal corresponding to a higher energy than the threshold. A rise-time discrimination technique [14] was employed to mitigate the impact of γ -rays. Furthermore, lead and poly blocks (as shown in the photograph in Fig. 4b) were employed to shield the detector from neutrons and γ -rays. Preliminary Monte Carlo simulations were conducted to validate the experiment's findings. The outcome of these simulations suggests that implementing successful cargo container scanning systems based on TENA using liquid scintillators would necessitate the incorporation of hundreds of kilograms of shielding materials around the detector [34,35,36]. This requirement presents a considerable challenge when attempting to adapt the TENA method with traditional detectors such as liquid scintillators and integrating it into a portable detection system.

Therefore, we are exploring alternative detector options that could enhance the method's reliability and enable its use in portable detection systems. By identifying and utilizing

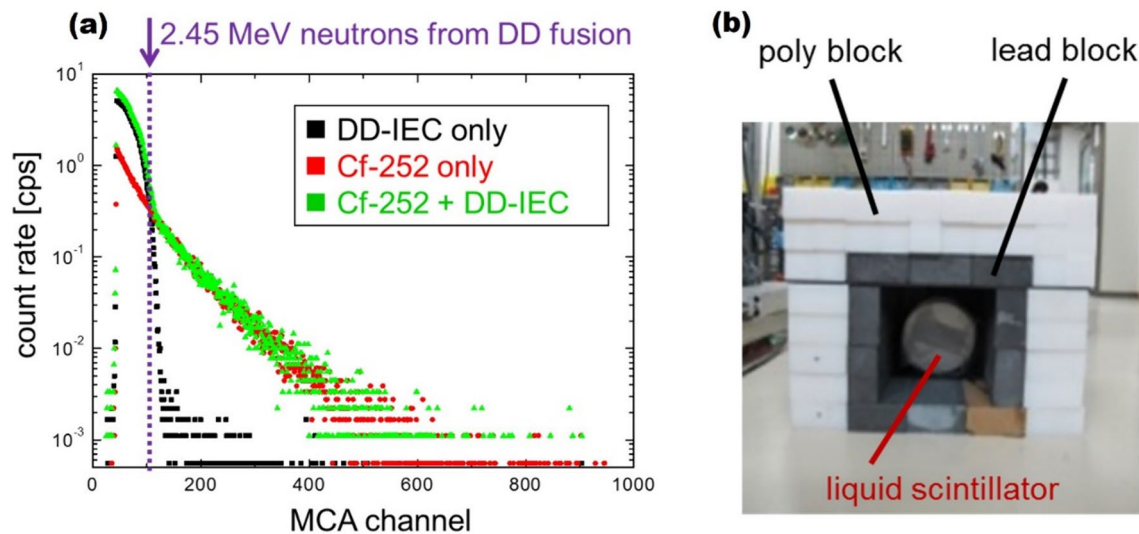


Fig. 4 (Color online) **a** Measured pulse high distributions by a liquid organic scintillator comparing three cases, namely with DD neutrons (black dots), a Cf-252 fission neutron source (red), and both of the

two simultaneously (green) [14]; **b** liquid organic scintillator inside the lead and poly blocks

more suitable detectors, the TENA technique can potentially become more practical and effective for various applications. The C-TMFD's capability to reject neutrons with energies below 2.45 MeV is harnessed to tackle the aforementioned challenge. The device is purposefully designed to operate at a threshold energy that aligns with the energy of the detected neutrons. This strategy ensures the efficient detection and identification of SNMs and the effective rejection of γ -rays. By aligning the threshold energy with that of the detected neutrons, the C-TMFD optimizes its performance, offering a reliable and precise means of detecting and distinguishing SNMs while effectively filtering out unwanted neutrons and γ -ray signals. This technological advancement holds the potential to considerably enhance the feasibility of utilizing the TENA method for various applications, including portable detection systems.

3 Experimental layout and conditions

A specific experimental setup was implemented to assess the efficacy of the TENA method, employing the C-TMFD as the neutron detector and an IEC fusion device as the DD neutron source for detecting HEU. This configuration included a bundle of six fission chambers (FCs) containing approximately 10 g of U-235 as the fissile material. Figure 5 visually depicts the experimental layout, illustrating the placement of the FCs housing HEU material, the IEC neutron source, and the C-TMFD neutron detectors. The C-TMFDs, labeled #1, #2, and #3, were positioned in close proximity to the FCs, fitting between the neutron source and the three C-TMFD detectors. The distance from the

center of the FCs to the center of the neutron generator was 55 cm, while the distances from the centers of the C-TMFDs, #1, #2, and #3, were 25 cm, 25 cm, and 40 cm, respectively, as demonstrated in Fig. 5a. The FCs and the C-TMFD sensors were placed on top of 5-cm-thick poly blocks, which likely served as a support structure and provided a consistent material background and neutron moderator for the measurements.

Before conducting the HEU detection experiments, preliminary scans without HEU were carried out to determine an appropriate induced tension value, denoted as p_{neg} , that would facilitate the exclusion of DD neutrons generated by the IEC device. The average neutron output from the IEC device was 3×10^5 n/s during the experiment campaigns. The results of these experiments are depicted in Fig. 6, where the vertical error bars in the count rate represent the statistical 1σ error, i.e., the square root of the measured count. A data point placed at zero count rate without an error bar indicates that no counts were observed within the 10 min measurement time. The horizontal axis, $p_{\text{neg},0} = p_{\text{neg}}(0)$, represents the induced tension on the rotation axis, with $r = 0$ in Eq. (1). The induced tension is not uniform and varies depending on the radial position within the detection volume. The measured count rates by the three C-TMFDs exhibit a rapid decrease as $p_{\text{neg},0}$ decreases to approximately 3.2 bar, followed by a gradual further decrease. This trend can be attributed to the spatial distribution of the induced tension, p_{neg} , within the detection volume, as well as the energy distribution of the incident neutrons, mainly due to scattering in the poly moderator.

For $p_{\text{neg},0} > 3.2$ bar in Fig. 6, the measured count rates by the respective C-TMFDs located at positions #1, #2,

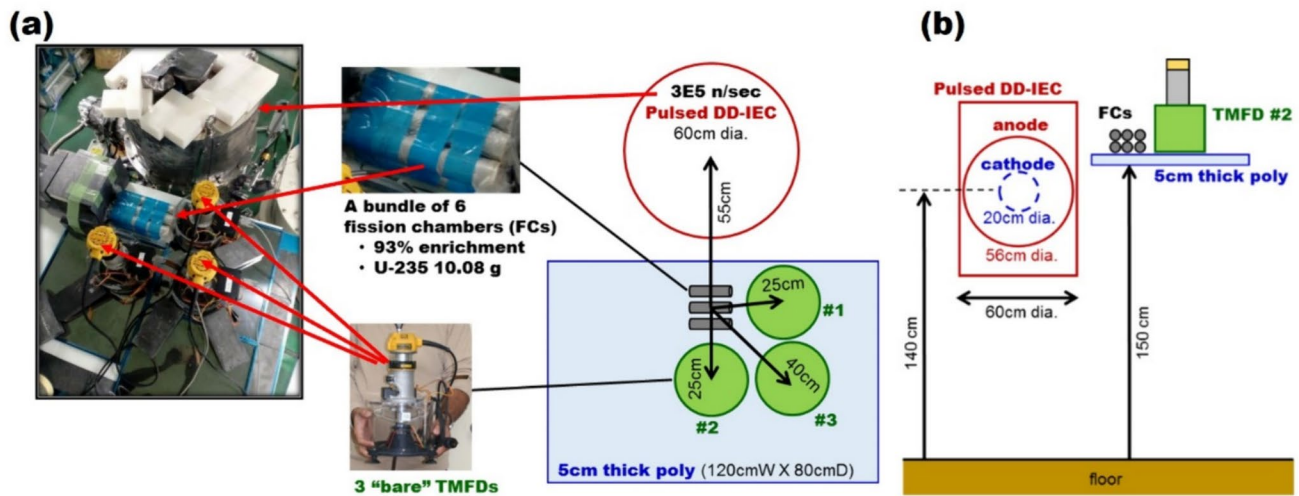


Fig. 5 (Color online) Experimental layout of a bundle of six fission chambers containing 10-g HEU in total, an IEC neutron generator, three TMFDs and poly moderators: **a** top view and **b** side view

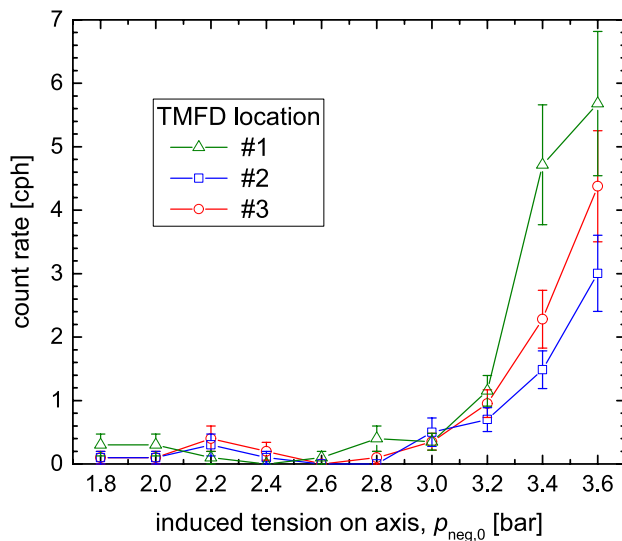


Fig. 6 (Color online) Measured count rates as a function of the induced tension in the C-TMFDs, without HEU, based on the experimental layout depicted in Fig. 5

and #3 (as shown in Fig. 5) follow the order $\#1 > \#3 > \#2$. This ranking is expected since the C-TMFD at position #1, being closest to the IEC neutron source, registers the highest count rate among the three. Additionally, the C-TMFD at position #3 records a higher count rate compared to #2, as the line of sight from the volumetric DD source to position #2 is more effectively blocked by the poly moderator than to position #3. However, below 3.0 bar, the count rate behavior observed for $p_{\text{neg},0} > 3.2$ bar is not maintained. This indicates that the low count

rates below 0.5 counts per hour (cph) might not result from neutrons generated by the IEC neutron source but rather be influenced by cosmic neutrons. Further investigation is required to study this in more detail in future studies. As the induced tension reduces, the threshold energy increases, decreasing the detection efficiency for fission neutrons [2]. However, the tension should be selected to ensure that the C-TMFD sensors are insensitive to the probing DD neutrons. Considering the results in Fig. 6, a $p_{\text{neg},0}$ value of 2.6 bar was chosen for the subsequent uranium detection experiments, assuming the C-TMFD sensors gate out the DD neutrons from the IEC source.

During the HEU interrogation test, a four-run campaign experiment was conducted, denoted as A to D. In this experiment, two runs were performed with HEU, and the other two runs were conducted without HEU. The measurement time for each run varied, with some lasting for 60 min and others for 30 min. The IEC neutron intensity remained consistent throughout the experiment at 3×10^5 n/s. Furthermore, the negative pressure of the C-TMFD was set to 2.6 bar. This test design allowed for a comprehensive assessment of the detection system's performance under different conditions, with and without the presence of HEU and varying measurement durations. The stability of the IEC neutron intensity and the chosen negative pressure in the C-TMFD ensured consistent and reliable experimental conditions across all four runs.

4 Results and discussion

Table 1 summarizes the experiment involving four sequential runs, with and without the FCs containing 10 g of HEU. The measurement time was 30 min for run C and 60 min for the remaining runs, excluding the dead time of the TMFD sensors. The measured counts by the three C-TMFDs (#1 to #3) during the four runs are presented in brackets in the following three columns. The resultant count rates in counts per hour are displayed in the corresponding cells without brackets. The count rates for TMFD #3, located 40 cm from the FCs, were normalized to the same distance of 25 cm as TMFD #1 and #2, using a normalization factor of $(40)^2/(25)^2$. Averages of the three normalized count rates are provided in the subsequent column, along with the 1σ statistical errors in the following right column. Upon comparing runs A and C (with HEU), the averaged normalized count rates (7.6 and 8.1 cph) show an agreement within the 1σ statistical error (2.0 or 3.0 cph). The same consistency is observed when runs B and D (without HEU) are compared; indicating the absence of significant systematic errors (e.g., temperature drift in the C-TMFD sensor liquid) affecting the count rates.

Comparing run A with HEU and run B without HEU reveals a clear difference between the two, namely 7.6 and 1.5 cph, respectively. The difference calculated as $(7.6-1.5)/(2.0+0.9)=2.1$ is shown in the rightmost column. This difference, exceeding 2σ , corresponds to more than a 96% confidence level in identifying the presence of HEU in run A. For runs C and D, the calculated difference is 1.4σ , smaller than that of runs A and B. This is reasonable since the detection time for run C is half, resulting in a larger statistical error. Both the averaged count rates for runs B and D without HEU are observed to be larger than the statistical errors, indicating the presence of a background source. Furthermore, when compared with the background level observed in Fig. 6, the background level in Table 1 appears to be higher. Further investigations are required in future to understand the source of this background, such as passive or active background from cosmic rays and/or from the DD neutron source. The low detection

efficiency in the preliminary experiment can be attributed to several factors. These include (i) the limited amount of U-235 used in the experiment, which was 10 g, (ii) the relatively low neutron intensity of 3×10^5 n/s employed during the test, and (iii) the need for optimization of C-TMFD-related parameters and positions. To improve the detection efficiency in the upcoming trial, a series of enhancements are planned. These include increasing the amount of HEU to over 70 g for interrogation, utilizing a higher neutron intensity of 5×10^7 n/s from the IEC source, operating under nominal neutron conditions, and assembling arrays of C-TMFDs that will undergo careful calibration to facilitate the experiment. Furthermore, a comprehensive calibration campaign is scheduled for the C-TMFD sensors. This campaign will encompass various calibration scenarios, including measurements with and without FCs, assessments with and without the presence of Cf-252, and a systematic scan to account for temperature effects on the sensors.

In an on-site inspection of a suspicious object, evaluating the background level is generally challenging as it depends on various factors inside the object and how many background neutrons and/or γ -rays are generated. Performing a separate test like run B or D without HEU is not feasible during an on-site nondestructive inspection. One potential advantage of the proposed TENA and C-TMFD-based scheme over other active methods is that background evaluation is possible if the background is predominantly owing to cosmic neutrons, as expected. Hence, a crucial next step is identifying the background source observed in Fig. 6 and Table 1. Understanding the background source is essential for accurate and reliable HEU detection using this method.

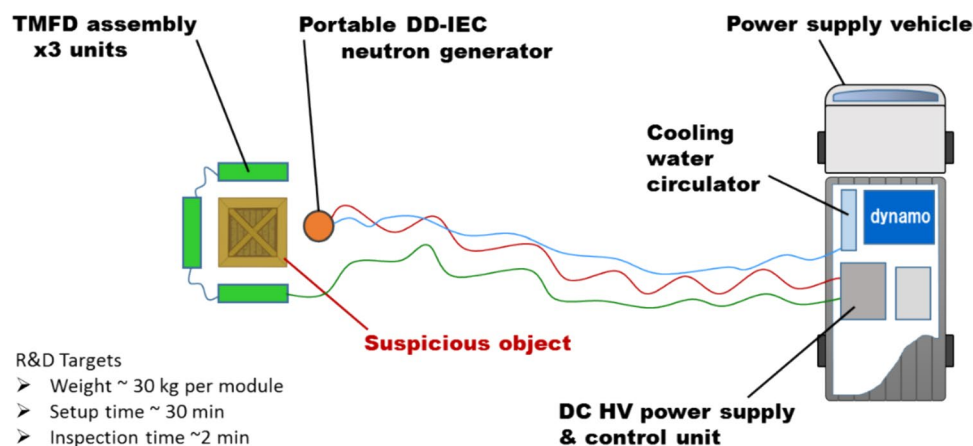
5 Plan

The R&D objective for the final product is to create a portable active interrogation system designed to detect SNMs. This system involves crew members wearing explosion-proof suits, enabling them to handle the neutron source and detector assembly modules with their hands. The weight of each module should be kept below 30 kg, the entire assembly

Table 1 The experimental count rates obtained from the TMFDs, both with and without FCs, in the configuration depicted in Fig. 6

Run No.	FCs (10 g HEU)	Time (min)	Normalized count rate, n (cph) and (actual count in brackets)				1σ Error in avg. norm. Count rate (cph)	$\frac{n_{\text{w}} - n_{\text{wo}}}{\sigma_{\text{w}} + \sigma_{\text{wo}}}$
			#1	#2	#3	Avg		
#A	With	60	06 (6)	9 (9)	07.7 (3)	7.6	2.0	2.1
#B	Without	60	01 (1)	2 (2)	N/a	1.5	0.9	
#C	With	30	10 (5)	4 (2)	10.2 (2)	8.1	3.0	1.4
#D	Without	60	03 (3)	2 (2)	02.6 (1)	2.2	1.1	

Fig. 7 (Color online) Schematic of the initial design concept for a portable, active, nondestructive interrogation system intended to detect SNMs



process completed within 30 min, and detection within 5 min. Figure 7 depicts the preliminary proposed concept for the portable active interrogation system based on the TENA method utilizing the C-TMFD technology and a portable neutron generator. To achieve this target, a portable (~ 30 kg net weight) and high-intensity neutron source developed from an IEC fusion device has been optimized and characterized to produce a neutron yield of approximately 10^8 n/s. This neutron source is ready for implementation during the second campaign for SNM interrogation. The capability of the C-TMFD sensors to effectively reject background neutrons and γ -rays without requiring additional shielding is crucial for minimizing the total weight and number of modules. To this end, the second generation of the C-TMFD (lightweight version) has been developed with a unit weight of 2.6 kg, ensuring that the total weight for a panel comprising nine units remains below 30 kg per module [2]. The proposed configuration for the C-TMFD sensors includes 27 units assembled into three modules, as illustrated in Fig. 7. The system also incorporates the necessary components to operate and control the neutron source, C-TMFD modules, and the TENA method detection process in one vehicle. Moreover, the control and monitoring of the C-TMFD modules are integrated into the setup.

Indeed, all components of the portable neutron interrogation system, including the C-TMFD sensors, power supply, cooling water circulators, control modules for the neutron source, and monitoring systems, are designed to be loaded onto a vehicle. This design allows the system to be transported and deployed at any location where a suspicious object is located, eliminating the need to bring the object to a laboratory for interrogation. This approach minimizes the risks associated with handling and moving the suspicious object, ensuring a safer and more efficient detection process. The system's portability enables it to be quickly deployed in various real-world scenarios, making it highly adaptable for detecting SNMs in different environments and situations. The optimization of the

system's design ensures that it remains lightweight and practical, offering an effective solution for SNM detection without compromising performance or reliability. This advancement marks a significant step toward enhancing the capability of nondestructive SNM detection in the field, where immediate and precise assessments are often crucial.

The second experimental campaign is scheduled to employ a recently developed IEC neutron source. In this setup, we will utilize 27 units of C-TMFDs organized into three modules. This campaign aims to interrogate natural uranium samples weighing 70 and 140 g. Various background scenarios will be considered to ensure a comprehensive analysis, including measurements with and without uranium in the setup, especially in cases where no D-D neutrons are generated from the IEC source. Furthermore, calibration and optimization of the neutron detectors will be performed. This calibration will involve using a Cf-252 neutron source and D-D neutrons generated by the IEC source. These steps are crucial for fine-tuning the neutron detectors' parameters and ensuring the measurements' accuracy.

6 Conclusion

A groundbreaking portable and nondestructive active interrogation system for SNMs is currently under development. A preliminary test was conducted using 10 g of HEU, and the results have shown great promise. This innovative system utilizes the TENA method to effectively distinguish fission neutrons, detected using the C-TMFD, from probing DD neutrons generated by the IEC neutron source. The experiments, employing approximately 10 g of HEU, three units of C-TMFDs, and an IEC neutron source producing 3×10^5 n/s DD neutrons, have demonstrated a reliable HEU detection capability with a 96% confidence level. This makes it a practical basis for a TENA-based interrogation system. The next phase involves integrating

three modules, consisting of 27 units of the lightweight version of C-TMFD, with the recently developed high-intensity and portable IEC neutron source for the second campaign aimed at detecting SNMs. This phase will include more scanned parameters and background analysis rejections for a comprehensive evaluation of the system's performance.

Acknowledgements This study has been conducted as a part of Projects to Support the Advancement of Strategic Core Technologies sponsored by Japan's Ministry of Economy, Trade and Industry (METI).

Author contributions All authors contributed to the study conception and design. Material preparation, data collection and analysis were performed by Mahmoud Bakr, Kai Masuda, Yoshiyuki Takahashi, Tsuyoshi Misawa, and Norio Yamakawa. The first draft of the manuscript was written by Mahmoud Bakr and Tomas Scott, and all authors commented on previous versions of the manuscript. All authors read and approved the final manuscript.

Declarations

Conflict of interest The authors declare that they have no conflict of interests.

Open Access This article is licensed under a Creative Commons Attribution 4.0 International License, which permits use, sharing, adaptation, distribution and reproduction in any medium or format, as long as you give appropriate credit to the original author(s) and the source, provide a link to the Creative Commons licence, and indicate if changes were made. The images or other third party material in this article are included in the article's Creative Commons licence, unless indicated otherwise in a credit line to the material. If material is not included in the article's Creative Commons licence and your intended use is not permitted by statutory regulation or exceeds the permitted use, you will need to obtain permission directly from the copyright holder. To view a copy of this licence, visit <http://creativecommons.org/licenses/by/4.0/>.

References

1. H. Ohgaki, T. Kii, K. Masuda et al., Proposal of a non-destructive detection system for hidden nuclear materials based on a neutron/gamma-ray hybrid system. *J. Korean Phys. Soc.* **59**, 3155–3159 (2011). <https://doi.org/10.3938/jkps.59.3155>
2. B. Archambault, A. Hagen, K. Masuda et al., Threshold rejection mode active interrogation of SNMs using continuous beam DD neutrons with centrifugal and acoustic tensioned metastable fluid detectors. *IEEE Trans. Nucl. Sci.* **64**, 1781–1788 (2017). <https://doi.org/10.1109/TNS.2016.2628244>
3. A. Murata, S. Ikeda, N. Hayashizaki, Design of an electron-accelerator-driven compact neutron source for non-destructive assay. *Nucl. Instrum. Meth. B* **406**, 260–263 (2017). <https://doi.org/10.1016/j.nimb.2016.12.024>
4. V.J. Orphan, E. Muenchau, J. Gormley et al., Advanced γ ray technology for scanning cargo containers. *Appl. Radiat. Isot.* **63**, 723–732 (2005). <https://doi.org/10.1016/j.apradiso.2005.05.033>
5. S. Fetter, V.A. Frolov, M. Miller et al., Detecting nuclear warheads. *Sci. Glob. Secur.* **1**, 225–253 (1990). <https://doi.org/10.1080/08929889008426333>
6. M.C. Hamel, J.K. Polack, M.L. Ruch et al., Active neutron and gamma-ray imaging of highly enriched uranium for treaty verification. *Sci. Rep.* **7**, 7997 (2017). <https://doi.org/10.1038/s41598-017-08253-x>
7. J.H. Sorebo, G.L. Kulcinski, R.F. Radel et al., Special nuclear materials detection using IEC fusion pulsed neutron source. *Fusion Sci Technol* **56**, 540–544 (2009). <https://doi.org/10.13182/FST56-540>
8. T. Gozani, Fission signatures for nuclear material detection. *IEEE Trans. Nucl. Sci.* **56**, 736–741 (2009). <https://doi.org/10.1109/TNS.2009.2015309>
9. W. Bertozzi, R.J. Ledoux, Nuclear resonance fluorescence imaging in non-intrusive cargo inspection. *Nucl. Instrum. Meth. B* **241**, 820–825 (2005). <https://doi.org/10.1016/j.nimb.2005.07.202>
10. J. Pruet, D.P. McNabb, C.A. Hagmann et al., Detecting clandestine material with nuclear resonance fluorescence. *J. Appl. Phys.* **99**, 123102 (2006). <https://doi.org/10.1063/1.2202005>
11. R.F. Radel, G.L. Kulcinski, R.P. Ashley et al., Detection of highly enriched uranium using a pulsed D-D fusion source. *Fusion Sci. Technol.* **52**, 1087–1091 (2007). <https://doi.org/10.13182/FST52-1087>
12. K.A. Jordan, T. Gozani, Detection of ^{235}U in hydrogenous cargo with differential die-away analysis and optimized neutron detectors. *Nucl. Instrum. Meth. A* **579**, 388–390 (2007). <https://doi.org/10.1016/j.nima.2007.04.083>
13. T. Misawa, Y. Takahashi, T. Yagi, et al., Development of measurement methods for detection of special nuclear materials using D-D pulsed neutron source. *Nuclear Physics Gamma-Ray Sources for Nuclear Security Nonproliferation*, pp 209–215 (2014). https://doi.org/10.1142/9789814635455_0025
14. M. Komeda, Y. Toh, Conceptual study on a novel method for detecting nuclear material using a neutron source. *Ann. Nucl. Energy* **135**, 106993 (2020). <https://doi.org/10.1016/j.anucene.2019.106993>
15. M. Komeda, Y. Toh, K. Tanabe et al., First demonstration experiment of the neutron rotation method for detecting nuclear material. *Ann. Nucl. Energy* **159**, 108300 (2021). <https://doi.org/10.1016/j.anucene.2021.108300>
16. R.L. Hirsch, Inertial-electrostatic confinement of ionized fusion gases. *J. Appl. Phys.* **38**, 4522–4534 (1967). <https://doi.org/10.1063/1.1709162>
17. R. Taleyarkhan, J. Lapinskas, Y. Xu, Tensioned metastable fluids and nanoscale interactions with external stimuli—theoretical-cum-experimental assessments and nuclear engineering applications. *Nucl. Eng. Des.* **238**, 1820–1827 (2008). <https://doi.org/10.1016/j.nucengdes.2007.10.019>
18. Y. Takahashi, T. Misawa, T. Yagi et al., Active neutron-based interrogation system with D-D neutron source for detection of special nuclear materials. In *Nuclear Physics Gamma-Ray Sources for Nuclear Security Nonproliferation* pp. 341–346 (2014). https://doi.org/10.1142/9789814635455_0041
19. R.L. Hirsch, Experimental studies of a deep, negative, electrostatic potential well in spherical geometry. *Phys. Fluids* **11**, 2486–2490 (1968). <https://doi.org/10.1063/1.1691842>
20. G.H. Miley, J. Sved, The IEC—a plasma-target-based neutron source. *Appl. Radiat. Isot.* **48**, 1557–1561 (1997). [https://doi.org/10.1016/S0969-8043\(97\)00257-1](https://doi.org/10.1016/S0969-8043(97)00257-1)
21. K. Masuda, R. Kashima, M.A. Bakr, Potential profile measurements inside a gridded cathode at high potential in a spherical inertial electrostatic confinement device. *Fusion Sci. Technol.* **75**, 608–613 (2019). <https://doi.org/10.1080/15361055.2019.1610292>
22. M. Bakr, J.P. Wulfkühler, K. Mukai et al., Evaluation of 3D printed buckyball-shaped cathodes of titanium and stainless-steel for IEC fusion system. *Phys. Plasmas* **28**, 012706 (2021). <https://doi.org/10.1063/5.0033342>
23. M. Bakr, T. Sakabe, J.P. Wulfkühler et al., Influence of electrodes' geometrical properties on the neutron production rate

- of a discharge fusion neutron source. *Phys. Plasmas* **30**, 032701 (2023). <https://doi.org/10.1063/5.0134631>
24. D.C. Donovan, D.R. Boris, G.L. Kulcinski et al., Measuring time of flight of fusion products in an inertial electrostatic confinement fusion device for spatial profiling of fusion reactions. *Rev. Sci. Instrum.* **84**, 033501 (2013). <https://doi.org/10.1063/1.4793771>
 25. J. Hedditch, R. Bowden-Reid, J. Khachan, Fusion energy in an inertial electrostatic confinement device using a magnetically shielded grid. *Phys. Plasmas* **22**, 102705 (2015). <https://doi.org/10.1063/1.4933213>
 26. N. Buzarbaruah, S.R. Mohanty, E. Hotta, A study on neutron emission from a cylindrical inertial electrostatic confinement device. *Nucl. Instrum. Meth. A* **911**, 66–73 (2018). <https://doi.org/10.1016/j.nima.2018.09.076>
 27. N. Matsui, T. Maegawa, K. Noborio et al., Neutronics analysis on the beam optics from cylindrical discharge type fusion device. *Fusion Sci. Technol.* **64**, 692–696 (2013). <https://doi.org/10.13182/FST13-A19173>
 28. T. Takamatsu, T. Fujimoto, K. Masuda et al., Spatial distribution of D-D neutrons from a compact water-cooled inertial electrostatic confinement device. *Fusion Sci. Technol.* **52**, 1114–1118 (2007). <https://doi.org/10.13182/FST07-A1647>
 29. J. Rasmussen, T. Jensen, S.B. Korsholm et al., Characterization of fusion plasmas in the cylindrical DTU inertial electrostatic confinement device. *Phys. Plasmas* **27**, 083515 (2020). <https://doi.org/10.1063/5.0013013>
 30. G.H. Miley, J. Javedani, Y. Yamamoto et al., Inertial-electrostatic confinement neutron/proton source. *AIP Conf. Proc.* **299**, 675–689 (1994). <https://doi.org/10.1063/1.2949222>
 31. K. Mukai, Y. Ogino, M.I. Kobayashi et al., Evaluation of tritium production rate in a blanket mock-up using a compact fusion neutron source. *Nucl. Fusion* **61**, 046034 (2021). <https://doi.org/10.1088/1741-4326/abe4e7>
 32. K. Masuda, K. Inoue, T. Kajiwara et al., Compact intense neutron generators based on inertial electrostatic confinement of D-D fusion plasmas. In *Nuclear Physics Gamma-Ray Sources Nuclear Security Nonproliferation*, pp. 195–202 (2014). https://doi.org/10.1142/9789814635455_0023
 33. H. Ohgaki, I. Daito, H. Zen et al., Nondestructive inspection system for special nuclear material using inertial electrostatic confinement fusion neutrons and laser Compton scattering gamma-rays. *IEEE Trans. Nucl. Sci.* **64**, 1635–1640 (2017). <https://doi.org/10.1109/TNS.2017.2652619>
 34. T. Sakabe, Y. Ogino, K. Mukai et al., Influence of the hydrogen isotope affinity of the cathode coating material on the neutron production rate in the glow discharge-type fusion neutron source. *Fusion Sci. Technol.* (2023). <https://doi.org/10.1080/15361055.2023.2227821>
 35. M. Bakr, K. Masuda, M. Yoshida, Development of a portable neutron generator based on inertial electrostatic confinement D-D fusion reaction. *AIP Con. Proc.* **2160**, 030004 (2019). <https://doi.org/10.1063/1.5127679>
 36. M. Bakr, K. Mukai, K. Masuda et al., Characterization of an ultra-compact neutron source based on an IEC fusion device and its prospective applications in radiography. *Fusion Eng. Des.* **167**, 112346 (2021). <https://doi.org/10.1016/j.fusengdes.2021.112346>